

Assessment of asymptotically corrected model potential scheme for charge-transfer-like excitations in oligoacenes

Wei-Tao Peng¹ and Jeng-Da Chai^{1,2,3,*}

¹*Department of Physics, National Taiwan University, Taipei 10617, Taiwan*

²*Center for Theoretical Sciences and Center for Quantum Science and Engineering,
National Taiwan University, Taipei 10617, Taiwan*

³*Physics Division, National Center for Theoretical Sciences (North),
National Taiwan University, Taipei 10617, Taiwan*

(Dated: August 15, 2014)

Abstract

We examine the performance of the asymptotically corrected model potential scheme on the two lowest singlet excitation energies of acenes with different number of linearly fused benzene rings (up to 5), employing both the real-time time-dependent density functional theory and the frequency-domain formulation of linear-response time-dependent density functional theory. The results are compared with the experimental data and those calculated by long-range corrected hybrid functionals and others. The long-range corrected hybrid scheme is shown to outperform the asymptotically corrected model potential scheme for charge-transfer-like excitations.

* Author to whom correspondence should be addressed. Electronic mail: jdchai@phys.ntu.edu.tw

I. INTRODUCTION

Over the past two decades, time-dependent density functional theory (TDDFT) [1] has been a popular method for the study of excited-state and time-dependent properties of large systems, due to its favorable balance between accuracy and efficiency [2, 3]. However, the exact exchange-correlation (XC) potential $v_{xc}(\mathbf{r}, t)$ in TDDFT remains unknown, and needs to be approximated for practical applications.

For a system subject to a slowly varying external potential, the most popular approximation for $v_{xc}(\mathbf{r}, t)$ is the adiabatic approximation,

$$v_{xc}(\mathbf{r}, t) \approx \left. \frac{\delta E_{xc}[\rho]}{\delta \rho(\mathbf{r})} \right|_{\rho(\mathbf{r})=\rho(\mathbf{r}, t)}, \quad (1)$$

where $v_{xc}(\mathbf{r}, t)$ is approximated by the functional derivative of the XC energy functional $E_{xc}[\rho]$ evaluated at the instantaneous density $\rho(\mathbf{r}, t)$. In the adiabatic approximation, memory effects, whereby $v_{xc}(\mathbf{r}, t)$ may depend on the density at all previous times ($t' < t$), are completely neglected. Surprisingly, results obtained from the adiabatic approximation can be accurate in many cases, even if the system considered is not in this slowly varying regime. However, as the exact $E_{xc}[\rho]$, which appears in both Kohn-Sham density functional theory (KS-DFT) [4] (for ground-state properties) and adiabatic TDDFT (for excited-state and time-dependent properties), has not been known, the development of a generally accurate density functional approximation for $E_{xc}[\rho]$ remains an important and challenging task [5, 6].

Functionals based on the localized model XC holes, such as the local density approximation (LDA) and generalized gradient approximations (GGAs), are reliably accurate for applications governed by short-range XC effects, such as low-lying valence excitation energies. However, they can produce erroneous results in situations where the accurate treatment of nonlocal XC effects is important. In particular, some of these situations occur in the asymptotic regions of atoms and molecules, where the LDA or GGA XC potential exhibits an exponential decay, instead of the correct $-1/r$ decay. Accordingly, LDA and GGAs (i.e., semilocal density functionals) severely underestimate high-lying Rydberg excitation energies [7–10], and completely fail for charge-transfer (CT) excitation energies [10–15] and excitations in completely symmetrical systems where no net CT occurs [16].

Aiming to resolve the asymptote problem, long-range corrected (LC) hybrid functionals [17–23] and asymptotically corrected (AC) model potentials [24–28], which are two distinct

density functional methods with correct asymptotic behavior, have been actively developed over the past few years. The LC hybrid scheme, which adopts 100% Hartree-Fock (HF) exchange for long-range electron-electron interactions, thereby provides an AC XC potential (i.e., a local multiplicative XC potential), when the optimized effective potential (OEP) method is employed [5, 29–31]. Similar to other orbital-dependent XC energy functionals, a generalized Kohn-Sham (GKS) method (i.e., using orbital-specific XC potentials) has been frequently employed in the LC hybrid scheme to circumvent the computational complexity of the OEP method, as the density, energy, and highest-occupied orbital energy obtained from the GKS method are generally similar to those obtained from the OEP method [5, 31]. In our recent work, the performance of the LC hybrid scheme (i.e., using the GKS method) and AC model potential scheme has been examined on a very wide range of applications [32]. In particular, we have shown that LC hybrid functionals could be reliably accurate for various types of excitation energies, including valence, Rydberg, and CT excitation energies, in the frequency-domain formulation of linear-response TDDFT (LR-TDDFT) [33]. Nevertheless, due to the inclusion of long-range HF exchange, the LC hybrid scheme can be computationally expensive for large systems.

On the other hand, in the AC model potential scheme, an AC XC potential is directly modeled, maintaining computational complexity similar to the efficient semilocal density functional methods. However, as most popular AC model potentials are found *not* to be functional derivatives [34, 35], the associated XC energies and XC kernels (i.e., the second functional derivative of $E_{xc}[\rho]$) are not well-defined. Accordingly, an adiabatic LDA or GGA XC kernel (i.e., *not* a self-consistent adiabatic XC kernel) has been frequently adopted for the LR-TDDFT calculations using the AC model potential scheme. Such combined approaches have been shown to perform well for both valence and Rydberg excitations, but very poorly for CT excitations [16, 32, 36–38], due to the lack of a space- and frequency-dependent discontinuity in the adiabatic LDA or GGA XC kernel adopted in LR-TDDFT [39]. Nevertheless, it remains unclear whether the AC model potential scheme can accurately describe CT or CT-like excitations, when a self-consistent adiabatic XC kernel (if available) is adopted in LR-TDDFT.

To circumvent this problem, in this work, we examine the performance of the AC model potential scheme on various types of excitation energies in the real-time formulation of TDDFT (RT-TDDFT), since LR-TDDFT is typically a good approximation to RT-TDDFT.

As an absorption spectrum (and hence, excitation energies) can be obtained by explicitly propagating the time-dependent Kohn-Sham (TDKS) equations, the knowledge of the XC kernel is not needed within the framework of RT-TDDFT. Particularly, we like to address if the AC model potential scheme is able to accurately describe CT-like excitations in RT-TDDFT, which to the best of our knowledge has never been addressed in the literature. The rest of this paper is organized as follows. In section II, we describe our test sets and computational details. The excitation energies calculated by the AC model potential scheme, the LC hybrid scheme, and others in both RT-TDDFT and LR-TDDFT are compared with the experimental data and the results obtained from a highly accurate *ab initio* method in section III. Our conclusions are given in section IV.

II. TEST SETS AND COMPUTATIONAL DETAILS

Linear n -acenes ($C_{4n+2}H_{2n+4}$), consisting of n linearly fused benzene rings (see Fig. 1), are important molecules for a variety of devices, such as organic light-emitting diodes [40], solar cells [41], and field-effect transistors [42]. Recently, the two lowest singlet $\pi \rightarrow \pi^*$ transitions of n -acenes, commonly labelled as the 1L_a (the lowest excited state of B_{2u} symmetry) and 1L_b (the lowest excited state of B_{3u} symmetry) states in Platt’s nomenclature [43], have received considerable attention [44–52].

The 1L_a state is dominated by a transition between the highest occupied molecular orbital (HOMO) and lowest unoccupied molecular orbital (LUMO), i.e., the HOMO \rightarrow LUMO transition, with polarization along the molecular short axis, while the 1L_b state is dominated by a combination of the two nearly degenerate configurations HOMO $- 1 \rightarrow$ LUMO and HOMO \rightarrow LUMO $+ 1$, with polarization along the molecular long axis. From a valence-bond point of view, the 1L_a state is mainly ionic in character, whereas the 1L_b state is mainly covalent in character [44, 45].

Kuritz *et al.* described the 1L_a state as a CT-like excitation [49], and showed that through a unitary transformation, the coupling between the HOMO and LUMO is weak, supporting the surmise of Richard and Herbert that the 1L_a state has CT character in disguise [48]. Note that as the 1L_a state is not a pure CT excitation (i.e., for well-separated donor-acceptor systems) [12, 13], the terminology “CT-like” may be controversial [46, 50, 52]. However, in this work, the 1L_a state is regarded as a CT-like excitation, as suggested in Refs. [48, 49]. By

contrast, the 1L_b state is a valence excitation with substantial double-excitation character [48]. In LR-TDDFT, although LDA and GGAs can accurately predict the 1L_b excitation energy, they substantially underestimate the 1L_a excitation energy [44–49, 51]. On the other hand, LC hybrid functionals are reliably accurate for the 1L_a state, but less accurate for the 1L_b state [46–49, 51]. Note that the efficient AC model potential scheme has never been examined on the 1L_a and 1L_b states of n -acenes in the literature.

To examine the performance of several density functional methods on various types of excitation energies in both RT-TDDFT and LR-TDDFT, the 1L_a and 1L_b states of n -acenes (up to 5-acene) are adopted as our test sets. For the LR-TDDFT calculations, we adopt LDA [53, 54], PBE [55] (a popular GGA functional), and LB94 [24] (a popular AC model potential) with the 6-31+G(d,p) basis set, to calculate the 1L_a and 1L_b excitation energies on the ground-state geometries of n -acenes obtained at the ω B97X/6-31G(d) level [19] with a development version of Q-Chem 4.0 [56]. For the LDA and PBE calculations, the adiabatic LDA and PBE XC kernels (i.e., the second functional derivatives of the LDA and PBE XC energy functionals, respectively) are adopted, respectively. For the LB94 calculations, the adiabatic LDA XC kernel is adopted, due to the lack of a self-consistent adiabatic XC kernel for the LB94 model potential.

The RT-TDDFT calculations, employing the adiabatic LDA, PBE, and LB94 XC potentials, are performed with the program package Octopus 4.0.1 [57]. The system, which is described on a real-space grid with a 0.2 Å spacing, is constructed by adding spheres created around each atom, of radius 6 Å. Troullier-Martins pseudopotentials are adopted to describe the complicated effects of the motion of core electrons [58]. To obtain spectroscopic information in RT-TDDFT, n -acene, which starts from the ground state, is excited via a linearly polarized delta kick in ν -direction:

$$v_{ext}(\mathbf{r}, t) = \hbar k \delta(t) r_\nu, \quad (2)$$

where r_ν is one of the Cartesian coordinates (x, y, z), and the perturbation strength $k = 0.01$ bohr $^{-1}$ is adopted to obtain linear spectroscopy [59]. To propagate the TDKS equations, we adopt a time step of $\Delta t = 0.001$ \hbar /eV (0.658 as) and run up to 100 \hbar /eV (65.8 fs), which corresponds to 10^5 time steps. The approximated enforced time-reversal symmetry (AETRS) algorithm is employed to numerically represent the time evolution operator [60].

III. RESULTS AND DISCUSSION

The absorption spectra of n -acenes, calculated by LDA, PBE, and LB94 in RT-TDDFT, are plotted in Figs. 2, 3, 4, and 5, where the spectra close to the position of the 1L_a and 1L_b peaks are highlighted in the subfigures, and the corresponding LR-TDDFT results are marked with the red lines. Note that the 1L_b state exhibits weak intensity compared with the 1L_a state. For 2-acene, as the oscillator strengths of the 1L_b state calculated by LDA, PBE, and LB94 in LR-TDDFT are found to be vanishingly small, the total propagation time adopted in our RT-TDDFT calculations may not be long enough to detect the 1L_b state.

For a comprehensive comparison, the 1L_a and 1L_b excitation energies, calculated by LDA, PBE, and LB94 in both RT-TDDFT and LR-TDDFT, are summarized in Tables I and II, respectively, where the results calculated by BNL [18] (a popular LC hybrid functional) are taken from Ref. [51], and those calculated by time-dependent coupled-cluster theory with single and double excitations (albeit with an approximate treatment of the doubles, CC2 [61]) and the experimental data are taken from Ref. [44].

Owing to the CT-like character, LDA and PBE significantly underestimate the excitation energies of the ionic 1L_a states in both RT-TDDFT and LR-TDDFT. Compared to the highly accurate CC2 results and experimental data, the errors of LDA and PBE increase with the acene length. LB94 performs similarly to LDA and PBE, indicating that the LB94 model potential is also inappropriate for CT-like excitations. As the LB94 results obtained from both the RT-TDDFT and LR-TDDFT calculations are very similar, the adiabatic LDA XC kernel adopted in the LR-TDDFT calculations appears to be appropriate. In RT-TDDFT, the failure of LB94 may be attributed to the lack of the step and peak structure in the adiabatic LB94 XC potential, which has recently been shown to be essentially important for CT excitations [62]. In LR-TDDFT, the failure of LB94 may be attributed to the lack of a space- and frequency-dependent discontinuity in the adiabatic LDA XC kernel adopted [11, 16, 37, 39]. Based on the above reasons, we expect that the CT failures may not be remedied by other AC model potentials exhibiting the same features as LB94 or a *pure* density functional whose functional derivative has the correct $-1/r$ asymptote [63]. By contrast, BNL performs very well on the excitation energies of the 1L_a states in both RT-TDDFT and LR-TDDFT. Fully nonlocal (i.e., orbital-dependent) functionals, in particular,

LC hybrid functionals, can be essential for the accurate description of CT-like excitations.

On the other hand, for the covalent 1L_b states, LDA, PBE, and LB94 accurately predict the 1L_b excitation energies in both RT-TDDFT and LR-TDDFT, yielding quantitative agreement with the experimental data. Due to the inclusion of a large fraction of HF exchange, BNL yields noticeable errors on the excitation energies of the 1L_b states in both RT-TDDFT and LR-TDDFT, which may be attributed to the pronounced double-excitation character of the 1L_b states [48]. It remains very difficult to accurately describe both the 1L_a and 1L_b states of n -acenes with existing density functionals.

IV. CONCLUSIONS

In this work, we have examined the performance of a variety of density functionals on the two lowest singlet $\pi \rightarrow \pi^*$ transition energies (i.e., the 1L_a and 1L_b states) of n -acenes (up to 5-acene) in both RT-TDDFT and LR-TDDFT. Our results have shown that the LB94 model potential performs similarly to LDA and PBE on both the 1L_a (CT-like) and 1L_b (valence) states. The excitation energies of the 1L_a states are severely underestimated by LDA, PBE, and the LB94 model potential, and the errors have been shown to increase with the acene length. Despite its computational efficiency, our results suggest that the LB94 model potential may not accurately describe CT-like excitations in both RT-TDDFT (due to the lack of the step and peak structure in the adiabatic LB94 XC potential) and LR-TDDFT (due to the lack of a space- and frequency-dependent discontinuity in the adiabatic LDA XC kernel adopted). Although only the LB94 model potential has been examined in this work, we expect that other AC model potentials exhibiting the same features as LB94 or a pure density functional whose functional derivative has the correct asymptote may not resolve the CT problems.

On the other hand, the LC hybrid scheme, which can be computationally expensive for large systems, is reliably accurate for the excitation energies of the 1L_a states due to the inclusion of long-range HF exchange, but less accurate for the excitation energies of the 1L_b states due to the significant double-excitation character of the 1L_b states. It remains very challenging to develop a generally accurate density functional for the ground-state, excited-state, and time-dependent properties of large systems.

ACKNOWLEDGMENTS

This work was supported by the National Science Council of Taiwan (Grant No. NSC101-2112-M-002-017-MY3), National Taiwan University (Grant No. NTU-CDP-103R7855), the Center for Quantum Science and Engineering at NTU (Subproject Nos.: NTU-ERP-103R891401 and NTU-ERP-103R891403), and the National Center for Theoretical Sciences of Taiwan.

-
- [1] E. Runge and E. K. U. Gross, *Phys. Rev. Lett.*, 1984, **52**, 997.
 - [2] M. A. L. Marques and E. K. U. Gross, *Annu. Rev. Phys. Chem.*, 2004, **55**, 427.
 - [3] C. A. Ullrich, *Time-Dependent Density-Functional Theory: Concepts and Applications*, Oxford University, New York, 2012.
 - [4] W. Kohn and L. J. Sham, *Phys. Rev.*, 1965, **140**, A1133.
 - [5] S. Kümmel and L. Kronik, *Rev. Mod. Phys.*, 2008, **80**, 3.
 - [6] A. J. Cohen, P. Mori-Sánchez, and W. Yang, *Chem. Rev.*, 2011, **112**, 289.
 - [7] M. E. Casida, C. Jamorski, K. C. Casida, and D. R. Salahub, *J. Chem. Phys.*, 1998, **108**, 4439.
 - [8] M. E. Casida and D. R. Salahub, *J. Chem. Phys.*, 2000, **113**, 8918.
 - [9] N. N. Matsuzawa, A. Ishitani, D. A. Dixon, and T. Uda, *J. Phys. Chem. A*, 2001, **105**, 4953.
 - [10] M. J. G. Peach, P. Benfield, T. Helgaker, and D. J. Tozer, *J. Chem. Phys.*, 2008, **128**, 044118.
 - [11] D. J. Tozer, *J. Chem. Phys.*, 2003, **119**, 12697.
 - [12] A. Dreuw, J. L. Weisman, and M. Head-Gordon, *J. Chem. Phys.*, 2003, **119**, 2943.
 - [13] A. Dreuw and M. Head-Gordon, *J. Am. Chem. Soc.*, 2004, **126**, 4007.
 - [14] B. M. Wong and J. G. Cordaro, *J. Chem. Phys.*, 2008, **129**, 214703.
 - [15] B. M. Wong, M. Piacenza, and F. D. Sala, *Phys. Chem. Chem. Phys.*, 2009, **11**, 4498.
 - [16] W. Hieringer and A. Görling, *Chem. Phys. Lett.*, 2006, **419**, 557.
 - [17] Y. Tawada, T. Tsuneda, S. Yanagisawa, T. Yanai, and K. Hirao, *J. Chem. Phys.*, 2004, **120**, 8425.
 - [18] R. Baer and D. Neuhauser, *Phys. Rev. Lett.*, 2005, **94**, 043002.
 - [19] J.-D. Chai and M. Head-Gordon, *J. Chem. Phys.*, 2008, **128**, 084106.

- [20] J.-D. Chai and M. Head-Gordon, *Phys. Chem. Chem. Phys.*, 2008, **10**, 6615.
- [21] T. Stein, L. Kronik, and R. Baer, *J. Am. Chem. Soc.*, 2009, **131**, 2818.
- [22] Y.-S. Lin, C.-W. Tsai, G.-D. Li, and J.-D. Chai, *J. Chem. Phys.*, 2012, **136**, 154109.
- [23] Y.-S. Lin, G.-D. Li, S.-P. Mao, and J.-D. Chai, *J. Chem. Theory Comput.*, 2013, **9**, 263.
- [24] R. van Leeuwen and E. J. Baerends, *Phys. Rev. A*, 1994, **49**, 2421.
- [25] P. R. T. Schipper, O. V. Gritsenko, S. J. A. van Gisbergen, and E. J. Baerends, *J. Chem. Phys.*, 2000, **112**, 1344.
- [26] D. J. Tozer, *J. Chem. Phys.*, 2000, **112**, 3507.
- [27] X. Andrade and A. Aspuru-Guzik, *Phys. Rev. Lett.*, 2011, **107**, 183002.
- [28] A. P. Gaiduk, D. S. Firaha, and V. N. Staroverov, *Phys. Rev. Lett.*, 2012, **108**, 253005.
- [29] R. T. Sharp and G. K. Horton, *Phys. Rev.*, 1953, **90**, 317.
- [30] J. D. Talman and W. F. Shadwick, *Phys. Rev. A*, 1976, **14**, 36.
- [31] S. Kümmel and J. P. Perdew, *Phys. Rev. B*, 2003, **68**, 035103.
- [32] C.-W. Tsai, Y.-C. Su, G.-D. Li, and J.-D. Chai, *Phys. Chem. Chem. Phys.*, 2013, **15**, 8352.
- [33] M. E. Casida, *Recent Advances in Density Functional Methods, Part I*, World Scientific, Singapore, 1995.
- [34] A. P. Gaiduk and V. N. Staroverov, *J. Chem. Phys.*, 2009, **131**, 044107.
- [35] A. P. Gaiduk and V. N. Staroverov, *Phys. Rev. A*, 2011, **83**, 012509.
- [36] D. J. Tozer, R. D. Amos, N. C. Handy, B. O. Roos, and L. Serrano-Andres, *Mol. Phys.*, 1999, **97**, 859.
- [37] O. Gritsenko and E. J. Baerends, *J. Chem. Phys.*, 2004, **121**, 655.
- [38] J. Neugebauer, O. Gritsenko, and E. J. Baerends, *J. Chem. Phys.*, 2006, **124**, 214102.
- [39] M. Hellgren and E. K. U. Gross, *Phys. Rev. A*, 2012, **85**, 022514.
- [40] M. A. Wolak, B. B. Jang, L. C. Palilis, and Z. H. Kafafi, *J. Phys. Chem. B*, 2004, **108**, 5492.
- [41] B. Walker, C. Kim, and T.-Q. Nguyen, *Chem. Mater.*, 2011, **23**, 470.
- [42] C. Wang, H. Dong, W. Hu, Y. Liu, and D. Zhu, *Chem. Rev.*, 2012, **112**, 2208.
- [43] J. R. Platt, *J. Chem. Phys.*, 1949, **17**, 484.
- [44] S. Grimme and M. Parac, *ChemPhysChem*, 2003, **3**, 292.
- [45] M. Parac and S. Grimme, *Chem. Phys.*, 2003, **292**, 11.
- [46] M. J. G. Peach, P. Benfield, T. Helgaker, and D. J. Tozer, *J. Chem. Phys.*, 2008, **128**, 044118.
- [47] B. M. Wong and T. H. Hsieh, *J. Chem. Theory Comput.*, 2010, **6**, 3704.

- [48] R. M. Richard and J. M. Herbert, *J. Chem. Theory Comput.*, 2011, **7**, 1296.
- [49] N. Kuritz, T. Stein, R. Baer, and L. Kronik, *J. Chem. Theory Comput.*, 2011, **7**, 2408.
- [50] M. J. G. Peach, M. J. Williamson, and D. J. Tozer, *J. Chem. Theory Comput.*, 2011, **7**, 3578.
- [51] K. Lopata, R. Reslan, M. Kowalska, D. Neuhauser, N. Govind, and K. Kowalski, *J. Chem. Theory Comput.*, 2011, **7**, 3686.
- [52] M. J. G. Peach and D. J. Tozer, *J. Phys. Chem. A*, 2012, **116**, 9783.
- [53] P. A. M. Dirac, *Proc. Cambridge Philos. Soc.*, 1930, **26**, 376.
- [54] J. P. Perdew and A. Zunger, *Phys. Rev. B*, 1981, **23**, 5048.
- [55] J. P. Perdew, K. Burke, and M. Ernzerhof, *Phys. Rev. Lett.*, 1996, **77**, 3865.
- [56] Y. Shao, L. Fusti-Molnar, Y. Jung, J. Kussmann, C. Ochsenfeld, S. T. Brown, A. T. B. Gilbert, L. V. Slipchenko, S. V. Levchenko, D. P. O'Neill, R. A. DiStasio Jr., R. C. Lochan, T. Wang, G. J. O. Beran, N. A. Besley, J. M. Herbert, C. Y. Lin, T. Van Voorhis, S. H. Chien, A. Sodt, R. P. Steele, V. A. Rassolov, P. E. Maslen, P. P. Korambath, R. D. Adamson, B. Austin, J. Baker, E. F. C. Byrd, H. Dachsel, R. J. Doerksen, A. Dreuw, B. D. Dunietz, A. D. Dutoi, T. R. Furlani, S. R. Gwaltney, A. Heyden, S. Hirata, C.-P. Hsu, G. Kedziora, R. Z. Khalliulin, P. Klunzinger, A. M. Lee, M. S. Lee, W. Liang, I. Lotan, N. Nair, B. Peters, E. I. Proynov, P. A. Pieniazek, Y. M. Rhee, J. Ritchie, E. Rosta, C. D. Sherrill, A. C. Simmonett, J. E. Subotnik, H. L. Woodcock III, W. Zhang, A. T. Bell, A. K. Chakraborty, D. M. Chipman, F. J. Keil, A. Warshel, W. J. Hehre, H. F. Schaefer III, J. Kong, A. I. Krylov, P. M. W. Gill, M. Head-Gordon, *Phys. Chem. Chem. Phys.*, 2006, **8**, 3172.
- [57] A. Castro, H. Appel, M. Oliveira, C. A. Rozzi, X. Andrade, F. Lorenzen, M. A. L. Marques, E. K. U. Gross, and A. Rubio, *Phys. Stat. Sol. B*, 2006, **243**, 2465.
- [58] N. Troullier and J. L. Martins, *Phys. Rev. B*, 1991, **43**, 1993.
- [59] K. Yabana, T. Nakatsukasa, J.-I. Iwata, and G. F. Bertsch, *Phys. Stat. Sol. B*, 2006, **243**, 1121.
- [60] A. Castro, M. A. L. Marques, and A. Rubio, *J. Chem. Phys.*, 2004, **121**, 3425.
- [61] O. Christiansen, H. Koch, and P. Jørgensen, *Chem. Phys. Lett.*, 1995, **243**, 409.
- [62] J. I. Fuks, P. Elliott, A. Rubio, and N. T. Maitra, *J. Phys. Chem. Lett.*, 2013, **4**, 735.
- [63] C.-R. Pan, P.-T. Fang, and J.-D. Chai, *Phys. Rev. A*, 2013, **87**, 052510.

TABLE I. Excitation energies (in eV) for the 1L_a states of n -acenes, calculated by various functionals in both RT-TDDFT and LR-TDDFT. The BNL results are taken from Ref. [51], and the CC2 and experimental results are taken from Ref. [44]. The mean absolute errors (MAEs) of these methods are provided for comparisons (error = theoretical value – experimental value).

n -acene	Experiment	CC2	RT-TDDFT				LR-TDDFT			
			LDA	PBE	LB94	BNL	LDA	PBE	LB94	BNL
2	4.66	4.88	4.11	4.11	4.12	4.79	4.16	4.16	4.09	4.86
3	3.60	3.69	2.96	2.97	2.97	3.68	3.00	3.01	2.96	3.72
4	2.88	2.90	2.20	2.22	2.21	2.91	2.25	2.26	2.21	2.94
5	2.37	2.35	1.67	1.70	1.69	2.41	1.71	1.73	1.69	2.39
MAE		0.09	0.64	0.63	0.63	0.07	0.60	0.59	0.64	0.10

TABLE II. Same as Table I, but for the 1L_b states of n -acenes.

n -acene	Experiment	CC2	RT-TDDFT				LR-TDDFT			
			LDA	PBE	LB94	BNL	LDA	PBE	LB94	BNL
2	4.13	4.46				4.61	4.29	4.29	4.21	4.64
3	3.64	3.89	3.65	3.64	3.68	4.03	3.69	3.69	3.61	4.07
4	3.39	3.52	3.26	3.26	3.28	3.68	3.29	3.30	3.23	3.70
5	3.12	3.27	3.00	2.99	3.01	3.42	3.03	3.03	2.97	3.44
MAE		0.22	0.09	0.09	0.09	0.37	0.10	0.10	0.11	0.39

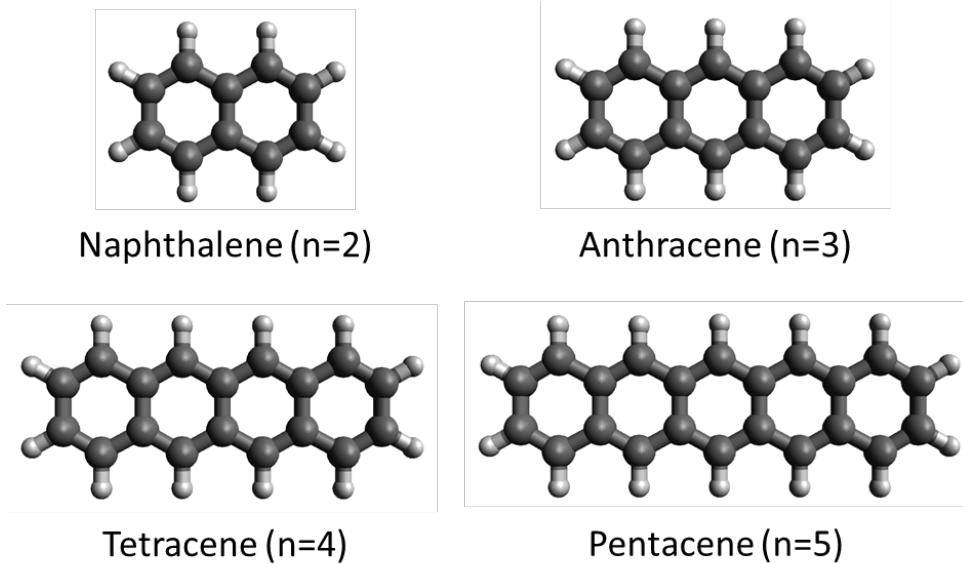


FIG. 1. Structures of the n -acenes investigated.

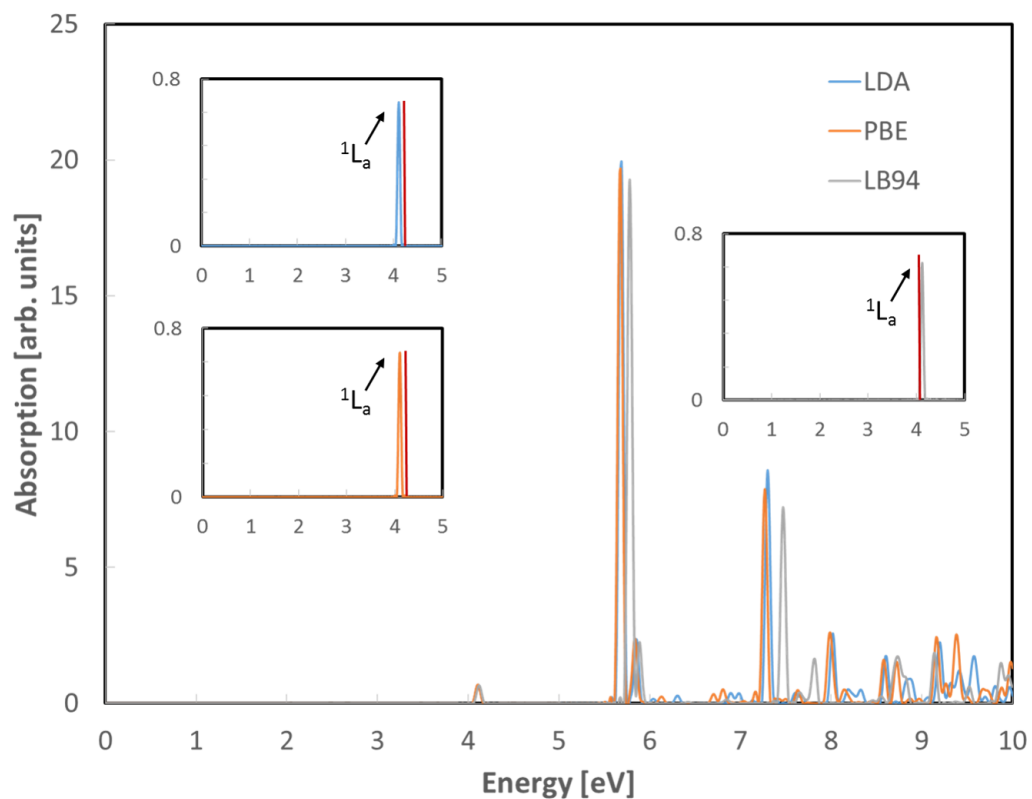


FIG. 2. Absorption spectra of 2-acene calculated by various functionals in RT-TDDFT. Subfigures (left top: LDA; left bottom: PBE; right: LB94) show the spectra close to the position of the $1L_a$ peaks, where the corresponding LR-TDDFT results are marked with the red lines.

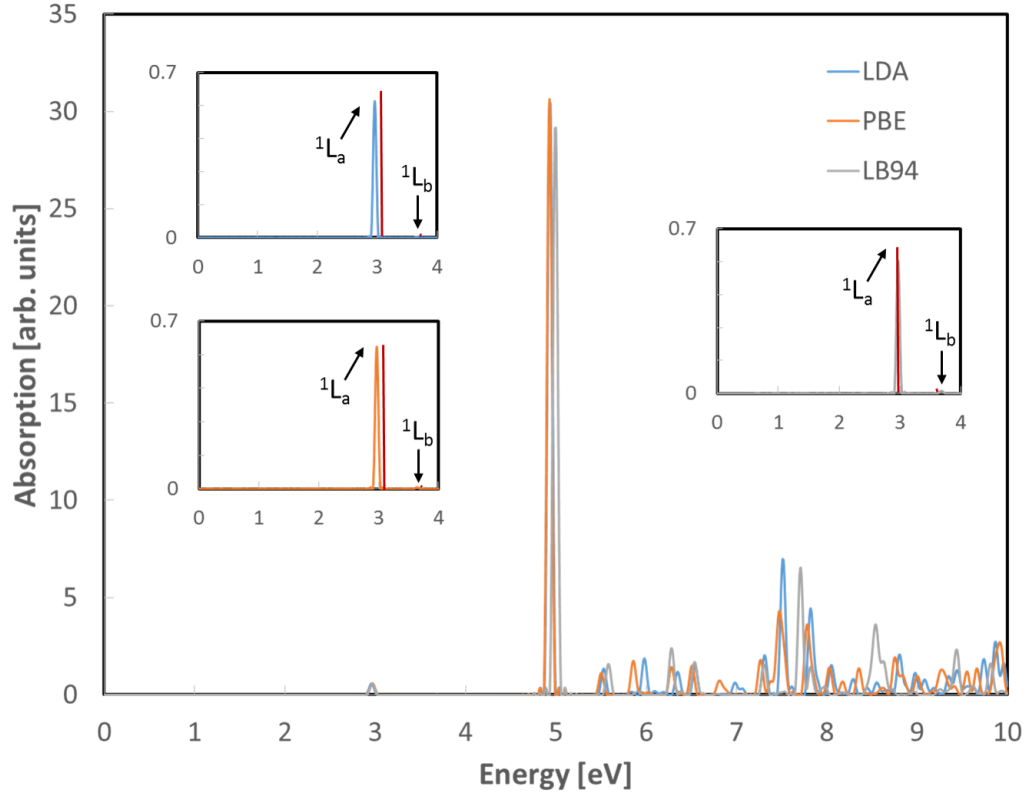


FIG. 3. Absorption spectra of 3-acene calculated by various functionals in RT-TDDFT. Subfigures (left top: LDA; left bottom: PBE; right: LB94) show the spectra close to the position of the 1L_a and 1L_b peaks, where the corresponding LR-TDDFT results are marked with the red lines.

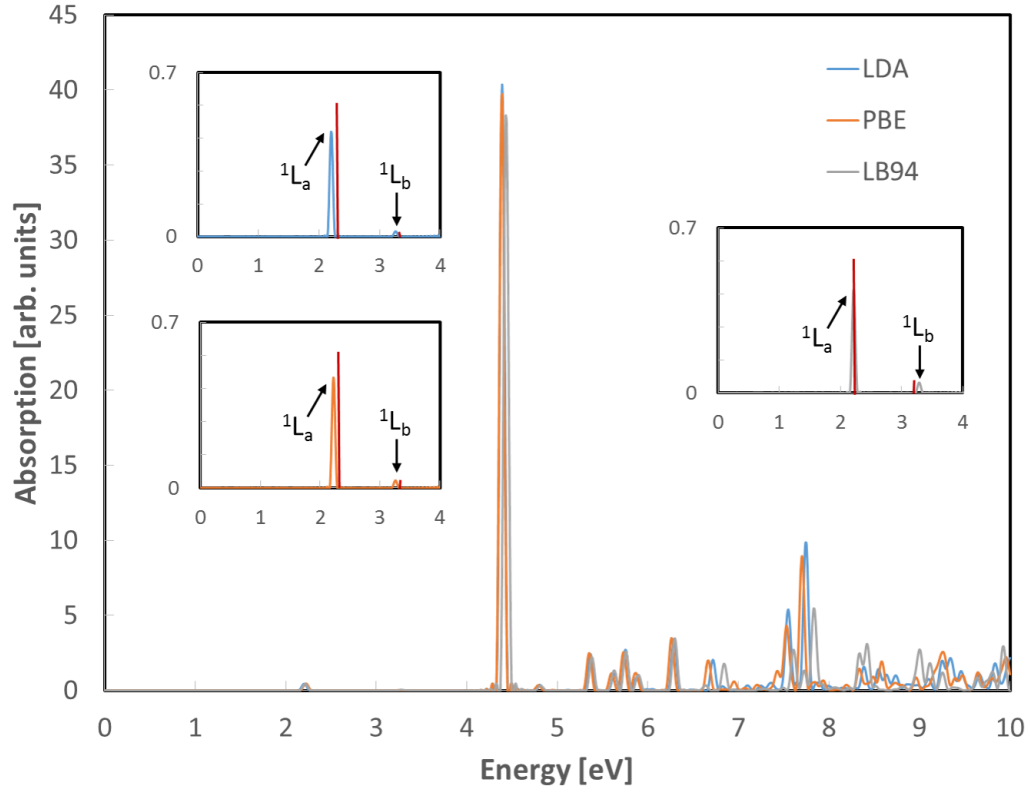


FIG. 4. Same as Fig. 3, but for 4-acene.

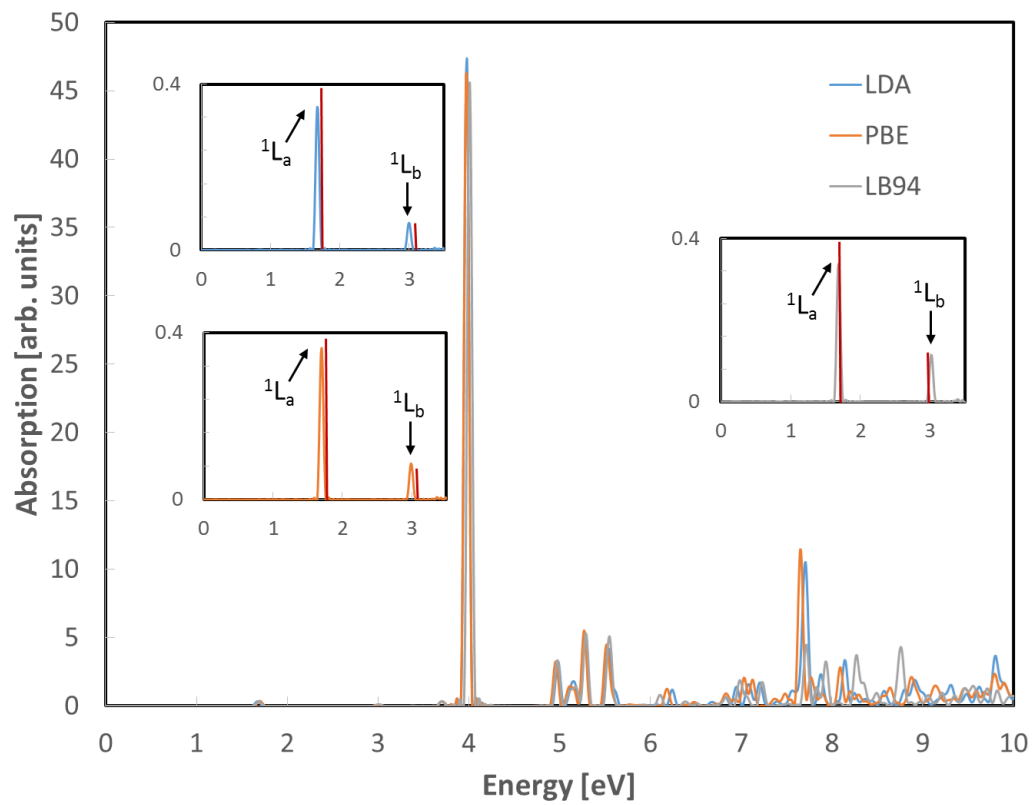


FIG. 5. Same as Fig. 3, but for 5-acene.